Applied Catalysis B: Environmental 199 (2016) 23–32

Contents lists available at ScienceDirect

Applied Catalysis B: Environmental

journal homepage: www.elsevier.com/locate/apcatb

Influence of boron addition to alumina support by kneading on morphology and activity of HDS catalysts

Yu.V. Vatutina*, O.V. Klimov, K.A. Nadeina, I.G. Danilova, E.Yu. Gerasimov, I.P. Prosvirin, A.S. Noskov

Boreskov Institute of Catalysis, Siberian Branch, Russian Academy of Sciences, pr. ak. Lavrentiev 5, 630090 Novosibirsk, Russia

ARTICLE INFO

Article history:
Received 2 March 2016
Received in revised form 18 May 2016
Accepted 4 June 2016
Available online 5 June 2016

Keywords:
Hydrotreating
Cobalt-molybdenum catalyst
Alumina
Boron
Acid properties

ABSTRACT

CoMo-catalysts modified by boron were studied. Boron was added to alumina support by kneading. Supports and catalysts were characterized by nitrogen adsorption, XPS, IR-spectroscopy of adsorbed CO. Catalysts were tested in hydrotreating of straight-run diesel fuel with 5 vol.% catalytic cracking gasoil (initial S content was 2750 ppm). It is found that boron has no significant influence on textural characteristics of catalysts. However, it increases slab length and visualization degree of active component, while stacking number remains unchanged (preferential formation of monolayers). Difference in morphology is caused by changes of Lewis acidity and generation of Brønsted acid sites. It is found that all catalysts with boron provide production of ultra-low sulfur diesel fuels (less than 10 ppm). The catalyst with a boron content of 2 wt.% combines high activity in HDS and HDN.

1. Introduction

Supported Co(Ni)-Mo hydrotreating catalysts are usually used to produce ultra-low sulfur diesel fuel. Active component of hydrotreating catalysts consists of Mo (or W) sulfide particles with cobalt (or nickel) atoms localized on its edges and corners [1]. Such active component is called CoMoS phase in the literature [2]. Numerous papers studied structure and properties of active component [1,3–7]. It was found that CoMoS phase of Type II with Co/(Co + Mo) = 0.3 was the most active [1]. Currently, there are many ways for selective synthesis of active component with definite structure.

γ-$A1_2O_3$ is usually used as a support of hydrotreating catalysts [8–10]. Its properties provide preparation of a support with desired porous structure, textural characteristics and mechanical strength [11]. However, increase of refining processing depth and toughening of ecological requirements for motor fuels causes a necessity to improve working characteristics of hydrotreating catalysts. For these purposes researchers often added different modifying agents to supports and catalysts, such as boron, silicon or phosphorous. Such additives are used in order to control the surface properties of the support and the dispersion and reactivity of the active phase. Rather contradictory data were obtained for boron influence on catalyst properties. Therefore, in this article, we paid attention on boron compounds [12–19].

The works devoted to the study of hydrotreating catalysts with boron revealed that introduction of boron provoked changes in the textural characteristics, the acidic properties of supports and catalysts, morphology of the sulfide active component and catalytic activity in HDS and HDN reactions [20–26].

In earlier work, Lafitau et al. studied [27] influence of boron on properties of $NiMo/Al_2O_3$ and found that boron decreased interaction between active component and a support. Decreased interaction resulted in higher HDS activity of catalysts for heavy fuels. On the contrary, investigation of Co/Al_2O_3 systems modified by boron [28,29] showed that boron causes increase of interaction of cobalt with a support. Therefore, formation of low active $CoAl_2O_4$ compounds was found that contradicted to the previous work. Changing the dispersity of active metals and their interaction with a support has been attributed to alteration of acid properties of a support. Indeed, alumina modified by boron has strong acidic properties as compared to alumina that makes it possible to use this system in cracking reactions [30]. Changing acidity associated with different interaction of boron with alumina. Thus, it was shown in Ref. [28] that increase of alumina acidity after boron addition occurs by the formation of Al-O-B-O-Al bonds. At the same

* Corresponding author.
E-mail address: yuliy.vatutina@yandex.ru (Yu.V. Vatutina).

http://dx.doi.org/10.1016/j.apcatb.2016.06.018
0926-3373/

time, the works [18,20,21,31] have shown that boron is uniformly distributed on the support surface without the formation of bulk particles of boric oxide. Formation of BO_3 occurs preferentially at low boron content (less than 0.3 wt.%) [21,23]. Concentration of BO_3 particles increases with boron content. Tetragonal BO_4 particles are formed at high boron loadings [21,24]. Formation of tetragonal BO_4 particles resulted in the increase of Brønsted acidity and strength of acid sites. Considerable increase of strength of acid sites was observed at 10 wt.% of B [32]. In addition, significant changes of Lewis acidity was revealed – decrease of amount of Lewis acid sites occurs after boron addition [21].

The literature data on textural characteristics are inconsistent and strongly depend on preparation method of supports and catalysts. Thus, there is a decrease of surface area and pore volume after impregnation of the support by boron compound [18,21]. In some cases, decrease or increase of surface area were observed at different boron content [33,34].

The data on the influence of boron on catalytic activity are also contradictory. Investigation of catalysts in hydrotreating of thiophene showed that optimal boron content to achieve high catalytic activity was 0.8 wt.% [18]. On the other hand, it was shown in Ref. [21] that there is no significant increase of catalytic activity after B addition. Moreover, boron content higher than 0.6 wt.% causes decrease of HDS activity. M. Lewandowski et al. [15] did not observe the effect of increasing the activity by adding boron.

It can be noted on the whole that differences observed in properties of supports and catalysts with the same content of modifying agent are caused by differences in preparation methods of catalysts. Particularly, there are an influence of method for introduction of modifying agent to a support, difference in initial reagents and conditions of catalysts preparation. All methods for boron introduction to catalyst given in the literature use preferentially impregnation method of support or catalyst by solution of boron compound. However, it requires an additional step in the catalyst preparation method.

In present work, influence of boron addition to alumina support by kneading has been studied. This method decreases amount of technological steps that is a priority when moving to the preparation method in industrial scale. Present work is devoted to the influence of boron on the formation of the active component, acidic and catalytic properties of Co-Mo hydrotreating catalysts diesel fractions.

2. Experimental

2.1. Preparation of supports

Boehmite produced by KNT-group (Ishimbay Specialized Chemical Plant of Catalysts, Ishimbay, Russia) was used as alumina precursor. It was shown recently [11] that morphology of its particles provided high mechanical strength of catalysts. HNO_3 was used as the peptizer agent. H_3BO_3 was used as a precursor of boron. Water solutions of HNO_3 and H_3BO_3 were added to boehmite powder in a Z-blade sigma mixer to prepare paste. Then the paste was extruded using a fluoroplastic spinneret with trilobular holes on the VINCI extruder. Trilobe and quadrilobe shapes of support granules are the most effective for deep hydrotreatment [35]. To provide an optimal diffusion of the feed along the catalyst granule, granules with a minimal volume-to-surface ratio and minimal granule diameter should be used. Therefore, granules in the form of trilobe extrudates with a cross-section diameter less than 1.5 mm were prepared in present work. After, granules were thermal treated at 110 °C for 2 h and 550 °C for 4 h in the air flow. Four samples with 1, 1.5, 2, 3 wt.% of boron were prepared. One sample without boron was prepared as a reference. Supports were denoted as Al-x, where x—wt.% of boron in a support.

2.2. Preparation of catalysts

Catalysts were prepared by vacuum impregnation technique. The supports were impregnated with the solution of bimetallic complex compound $[CoL]_2[Mo_4(C_6H_5O_7)_2O_{11}]\cdot nH_2O$, where L is NH_3 or H_2O. The synthesis of this compound was described in details in our previous work [36]. Impregnation and drying techniques were described in Ref. [37]. Catalysts were dried at 120°C for 4 h in air flow. In all instances, concentrations of impregnating solutions were chosen to obtain 10.0 ± 0.1 wt.% of Mo and 3.0 ± 0.1% of Co. Hereinafter catalysts are designated as CoMo/Al-x, where x—wt.% of boron in a support.

2.3. Sulfiding and testing of catalysts

The catalysts were crushed to a particle size of 0.25–0.5 mm. Sulfiding was performed with a dimethyl disulfide solution (20 g/L) in a straight-run diesel fuel with 0.3 wt.% of sulfur in the following conditions: a pressure of 3.5 MPa, a volumetric hydrogen/sulfiding mixture ratio of 300 and a stepwise elevated temperature (140, 240, 340 °C). This method is similar to the sulfiding techniques used at actual refinery plants.

Catalysts were tested in hydrotreating of straight-run diesel fraction (AO "Gazpromneft-Omskii NPZ", Omsk, Russia) that was mixed with 5 vol.% of catalytic cracking gasoil. Catalyst weight was 4 g. Process parameters were the following: P = 3.8 MPa, H_2/feed = 396 nm^3/m^3, LHSV = 1.9 h^{-1}, T = 340 °C, 350 °C, 360 °C. For each temperature, liquid samples of the first 6 h were not taken, since this period was necessary for catalysts to reach a stationary state. During the next 6 h samples were analysed and the obtained results were averaged out. As a rule, differences in the measured sulfur content did not exceed 5 ppm. Sulfur and nitrogen concentrations in the feed were 2750 ppm and 125 ppm, respectively. The sulfur content in the liquid products was measured by TE Instruments XPLORER. Difference between sulfur content in steady state was no more than 1 ppm. Difference in residual sulfur content for each HDS point was in precision of measurement for TE Instruments XPLORER. Uncertainty of measurements for our sulfur content is 2% (less than 0.5 ppm). General uncertainty for testing was ±1.5 ppm.

3. Investigation techniques

3.1. Nitrogen adsorption-desorption

The textural properties of the catalysts and supports were determined by nitrogen physisorption using an ASAP 2400 (USA) instrument. Prior to analysis, samples were subjected to a N_2 flow at 200 °C for 2 h. The BET surface areas were calculated from the nitrogen uptakes at relative pressures ranging from 0.05 to 0.30. The total pore volume was derived from the amount of nitrogen adsorbed at a relative pressure close to unity (in practice, P/P0 = 0.995) by assuming that all accessible pores had been filled with condensed nitrogen in the normal liquid state. The pore size distribution was calculated using the BJH method using the adsorption and desorption branches of the isotherm.

3.2. HRTEM

HRTEM images were obtained by a JEM-2010 electron microscope (JEOL, Japan) with a lattice-fringe resolution of 0.14 nm at an accelerating voltage of 200 kV. The high-resolution images of the periodic structures were analysed by the Fourier method. Samples for HRTEM examination were prepared on a perforated carbon

film mounted on a copper grid. The particle size of the initial AlOOH powders and the slab length of the sulfide active component were defined using the average data for at least 500 particles.

3.3. XPS

X-ray photoelectron spectra (XPS) were recorded using a SPECS spectrometer (Germany) with a PHOIBOS-150 hemispherical energy analyser and Al Kα irradiation (hν = 1486.6 eV, 200 W). The binding energy scale was preliminarily calibrated using the peak positions of the Au4f7/2 (84.0 eV) and Cu2p3/2 (932.67 eV) core levels. The samples were supported using conductive scotch tape. The internal reference method was used for the correct calibration of the photoelectron peaks. Al2p (E_b = 74.6 eV) and Al2 s (E_b = 119.4 eV) lines were used for calibration. A low-energy electron gun (FG-15/40, SPECS) was used for the sample charge neutralization.

3.4. IR-spectroscopy of adsorbed CO

The surface acid Lewis and Brønsted sites of the samples were studied by IR spectroscopy of adsorbed carbon monoxide. IR spectra of adsorbed CO were recorded by Shimadzu FTIR-8300 spectrometer within the spectral range of 700–6000 cm^{-1} with a resolution of 4 cm^{-1} and 300 scans for signal accumulation. The powder samples were pressed into thin self-supporting wafers (0.010–0.014 g/cm^2) and activated in the special IR cell at 773 K for 1 h in air and further at 823 K for 2 h in dynamic vacuum of 10^{-3} mbar. CO was introduced at liquid nitrogen temperature by doses (200–300 μmol g−1) up to an equilibrium pressure of 10 mbar and following desorption was performed by heating to room temperature. An increase in the frequency of the ν(CO) band of CO adsorbed relative to the value of free CO molecules (2143 cm^{-1}) is caused by the formation of complexes with Lewis (LAS) or Brønsted acidic sites (BAS). Complexes with LAS are characterized by the bands with the frequency above 2178 cm^{-1}, whereas the frequency range from 2150 through 2178 cm^{-1} is typical for complexes of CO with OH-groups. After deconvolution of the corresponding IR bands into individual Gauss components by home-made program, the concentration of Lewis acidic sites (LASs) was evaluated from the integral intensity (A) of CO band in the range of 2178–2233 cm^{-1} using the equation: C = A/A0. The following molar integral absorption coefficients values (A0, cm/μmol) determined for unmodified Al_2O_3 were used: 1.23 (2233–2225 cm^{-1}), 1.1 (2218–2208 cm^{-1}), 0.9 (2192–2178 cm^{-1}) [38,39]. A value of the upward νCO frequency shift determines the strength of Lewis acid sites, as it is related to the heat of complex formation by the following formula: QCO [kJ/mol] = 10.5 + 0.5(νco-2143) [20]. The strength of Bronsted acid sites (BASs) was estimated by the method of hydrogen bonds based on the change in the stretching vibration frequency of the OH groups that occurred under CO absorption (Δ νOH) [38,39]. The higher the shift of OH stretching vibration, the stronger the acidity of this OH-group. The concentration of BASs were determined from the intensity of the bands attributed to corresponding OH-group in the H-complex with the CO molecule. In the presented spectra, the absorbance was normalized to sample wafer density.

4. Results

4.1. Textural characteristics

Textural characteristics of the supports and catalysts are given in Table 1. Adding of boron has no significant influence on average pore volume and surface area of supports and catalysts. Increase of boron content causes the slight increase of surface area from 211 to 233 m^2/g. However, values of surface area for the catalysts are similar.

Table 1
Textural characteristics of supports and catalysts.

Boron concentration (wt.%)	Surface area (m^2/g)		Pore volume (cm^3/g)	
	support	catalyst	support	catalyst
0	211	176	0.53	0.41
1	218	168	0.54	0.43
1.5	221	168	0.53	0.39
2	222	176	0.53	0.41
3	233	158	0.53	0.39

Table 2
HRTEM data for sulfide catalysts.

Catalyst	Average slab length (nm)	Average stacking number	Average number of layers per 1000 nm^2
CoMo/Al-0	3.1	1.2	35
CoMo/Al-1	3.8	1.1	43
CoMo/Al-1.5	3.5	1.1	45
CoMo/Al-2	3.5	1.2	50
CoMo/Al-3	3.4	1.2	49

Examples of pore size distributions for supports and catalysts with 0 and 2 wt.% of B are given in Fig. 1. Pore size distributions of other samples are similar. All catalysts and supports have narrow pore size distribution. There is no significant amount of micropores in initial supports and final catalysts. The most part of pores in supports have the diameters in the range of 7–13 nm. According to Ref. [40], these pores have a positive influence on catalytic activity. After impregnation, a pore volume for pores with the diameters of 7–13 nm decreases. Subsequently, active component particles localize in these pores.

Nitrogen adsorption-desorption isotherms for the supports and catalysts with 0 and 2 wt.% of B are given in Fig. 2. All isotherms are attributed to IV type with hysteresis loops of type H1 [41]. It is typical for mesoporous supports and catalysts with cylindrical type of pores. The form of hysteresis loops does not change after impregnation of supports. It indicates that the form of pores for the supports and catalysts is similar. Therefore, there is no plugging of pores by active component particles.

4.2. HRTEM

Rather amount of HRTEM images for each catalyst were investigated for analysis of active component morphology. Conclusions about differences between CoMoS phase and MoS_2 have been made due to statistical data of previous works [36,37,42]. To analyze catalyst surface, sufficient amount of HRTEM images was recorded at different microscope focusing. Then, all these images have been studied. No unsulfided particles are observed. HRTEM images of the typical surface fragments of the sulfide CoMo/Al-x catalysts are given in Fig. 3. Active component particles have a morphology that is similar to the Co-Mo-S phase in high active hydrotreating catalysts [43,44]. Active phase is uniformly distributed in the catalysts. There are no seen bulk individual sulfides of Co or Mo. Average stacking number, average slab length and number of layers per 1000 nm^2 were calculated for all catalysts. The results are given in Table 2. It was noted that addition of boron into catalyst support resulted in the increase of average slab length. However, dependence of slab length on boron content is nonlinear. Addition of 1 wt.% of boron results in the increase of slab length to 3.8. Further increase of boron content causes the decrease of average slab length from 3.8 to 3.4 nm, while average stacking number remains unchanged. It should be noted that catalysts with B contain more

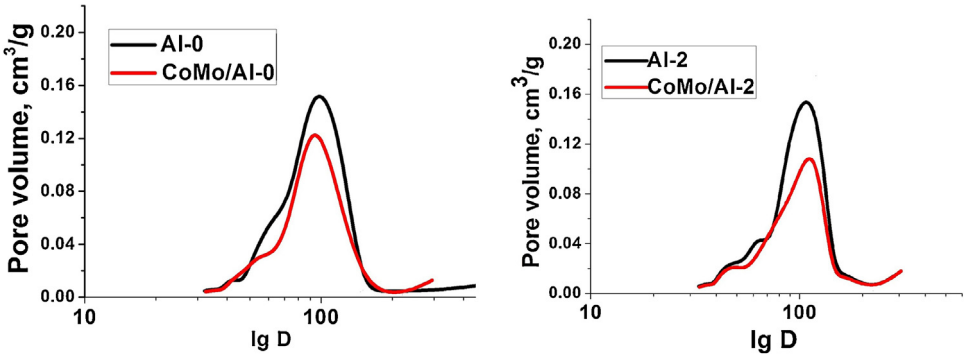

Fig. 1. Pore size distribution for supports and catalysts with 0 and 2 wt.% of B.

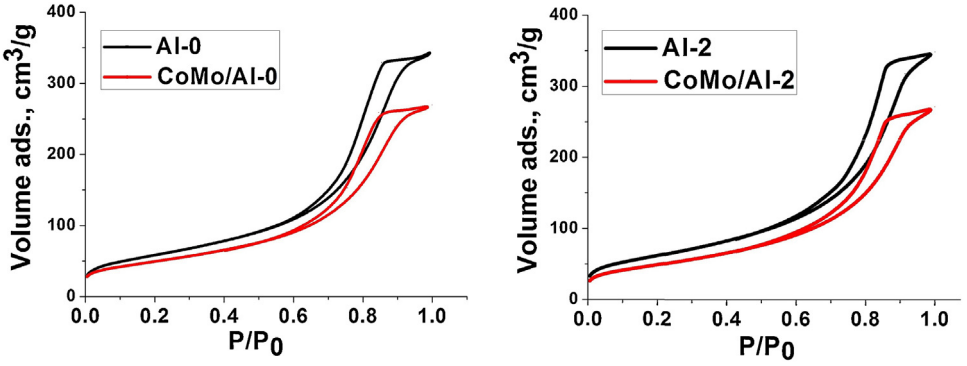

Fig. 2. Nitrogen adsorption-desorption isotherms for supports and catalysts with 0 and 2 wt.% of B.

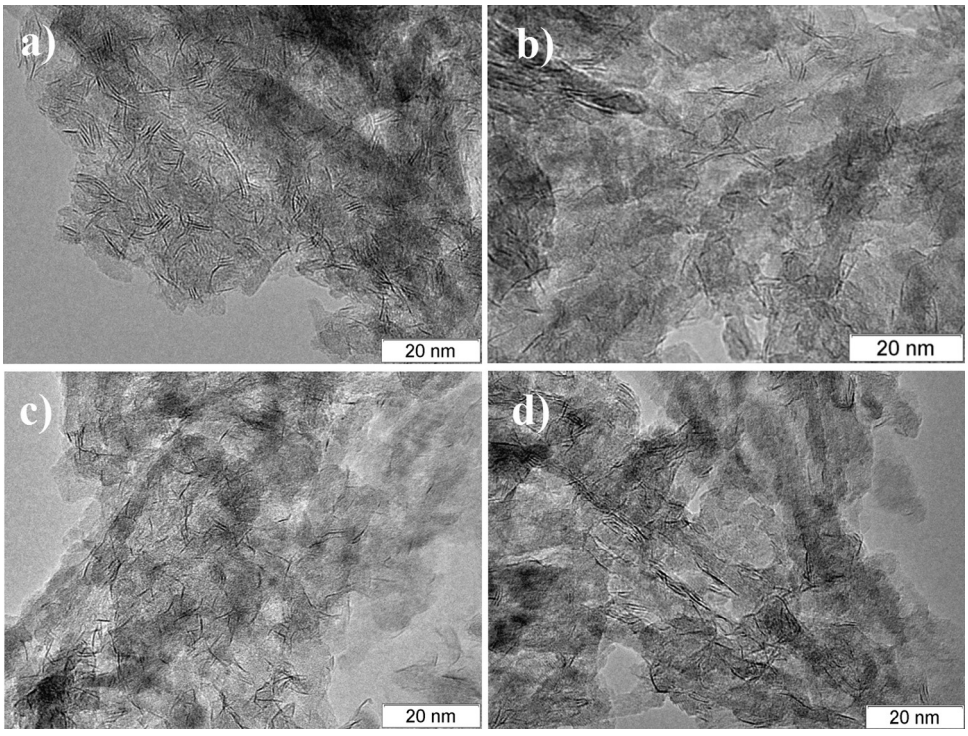

Fig. 3. TEM patterns by typical part of modified sulfide samples catalysts: (a) CoMo/Al-1, (b) CoMo/Al-1,5, (c) CoMo/Al-2, (d) CoMo/Al-3.

active component that is visible in HRTEM images, while active metals content is similar for all catalysts. CoMo/Al-0 catalyst contains 35 slabs per 1000 nm^2, while B containing ones have more than 40 slabs per 1000 nm^2. CoMo/Al-2 catalyst contains the highest amount of visible slabs.

Table 3
XPS data for sulfide catalysts.

	CoMo/Al-0	CoMo/Al-1	CoMo/Al-1.5	CoMo/Al-2	CoMo/Al-3
BE, Mo3d (eV)	229.1	229.1	229.1	229.1	229.1
Mo^{4+} (%)	89	70	73	75	72
Mo^{5+} (%)	6	16	14	14	17
Mo^{6+} (%)	5	14	13	11	11
BE, Co2p (eV)	779.0	779.0	779.0	779.0	779.0
CoMoS (%)	75	60	58	71	62
Co^{2+} (%)	25	40	42	29	38
BE, S2p (eV)	161.7	161.7	161.7	161.7	161.7
B1s	–	192.7	192.7	192.7	192.7
Mo/Al	0.11	0.13	0.12	0.12	0.12
Co/Al	0.02	0.05	0.04	0.04	0.04
B1s/Al2p	–	0.03	0.13	0.06	0.06

	ΔBE, eV—evidence this research	ΔBE, eV—[49]	ΔBE, eV—[32]
Co2p-Mo3d	549.9	549.8	550
Co2p-S2p	617.3	617.1	616.8

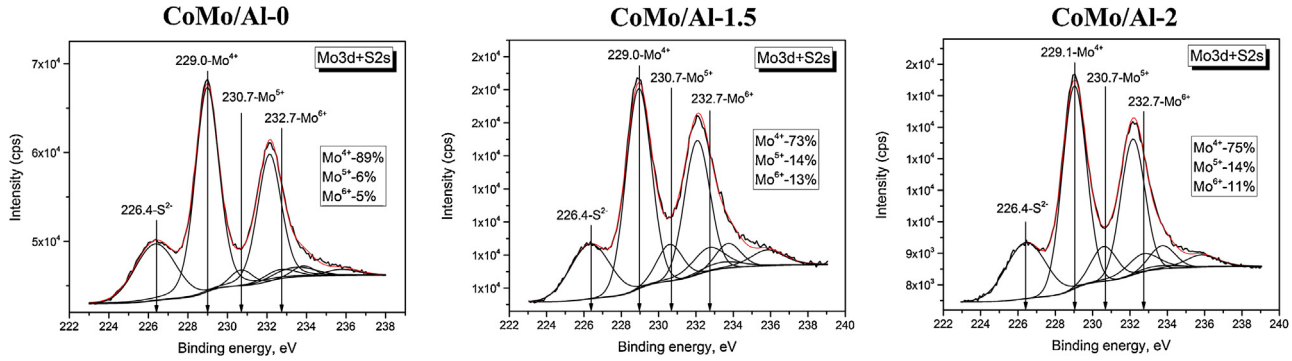

Fig. 4. Decomposition of Mo3d on Mo^{4+}, Mo^{5+}, Mo^{6+} for CoMo/Al-0, CoMo/Al-1.5 and CoMo/Al-2.

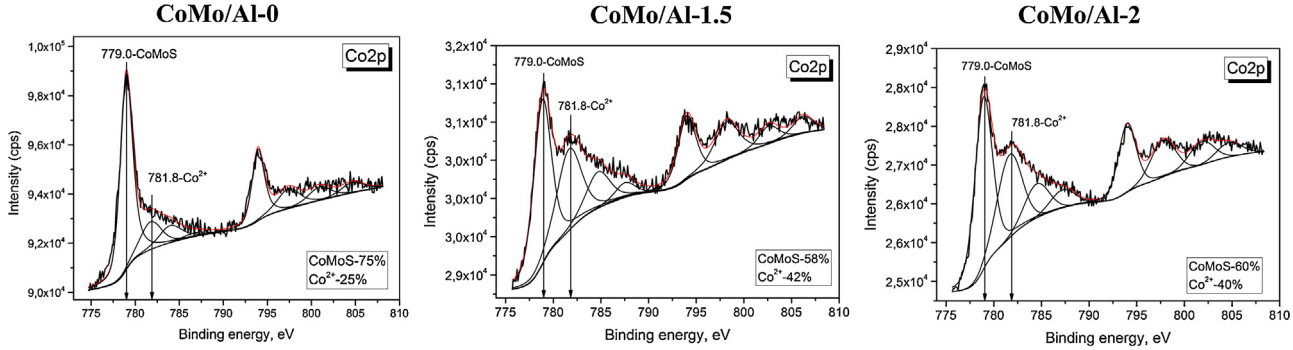

Fig. 5. Decomposition of Co2p spectra on CoMoS, Co^{2+} for CoMo/Al-0, CoMo/Al-1.5 and CoMo/Al-2.

4.3. XPS

XPS spectra of Mo3d, S2p, Co2p, B1s were obtained for all catalysts. Surface concentrations for molybdenum, cobalt, boron and sulfur were calculated. Binding energies (BE) and concentration of different states of Mo and Co are given in Table 3. Mo3d spectra of the catalysts contain peaks with similar intensity and width. Deconvolution of Mo3d spectra was made to define molybdenum state. Examples of spectra deconvolution for CoMo/Al-0, CoMo/Al-1.5 and CoMo/Al-2 are given in Fig. 4. The results for other catalysts are similar. The peak of the highest intensity with the binding energy of 229.1 eV is attributed to Mo^{4+} state. It is in a good accordance with Refs. [11,45–47] for Mo in the composition of Co-Mo-S phase. The binding energy at 232.7 eV is characterized for Mo^{6+} that is typical for MoO_3 [46]. Resulting concentrations of different Mo states in the catalysts are in the following range: Mo^{4+}—70–89%, Mo^{5+}—6–17%, Mo^{6+}—5–14%.

Deconvolutions of Co2p spectra for CoMo/Al-0, CoMo/Al-1.5 and CoMo/Al-2 are given in Fig. 5. The results of deconvolution for other catalysts are similar. The binding energy value at 779.1 eV of the most intensive peak corresponds to Co^{2+} in the composition of the Co-Mo-S phase [11,42,46,48–50]. The binding energy value at 781.8 eV is typical for Co^{2+} in Co-O [11,50]. Contents of different Co states in the catalysts are in the following range: Co in the composition of Co-Mo-S—58–75% and Co-O—28–42%. In addition, ΔBE[Co2p-Mo3d], ΔBE[Co2p-S2p] and ΔBE[Mo3d-S2p] were calculated. Resulting values—549.9 eV, 617.3 eV and 67.4 eV, respectively, are in accordance with the data for Co-Mo-S phase [47,49]. The peaks with BE 161.7 eV and 163.1 eV are observed in the S2p spectra for all samples (Fig. 6). These binding energies are

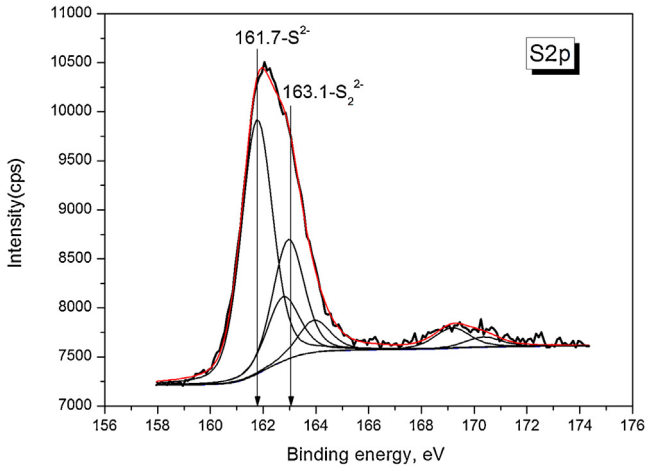

Fig. 6. Decomposition of S2p spectra on S^{2-}, S_2^{2-}.

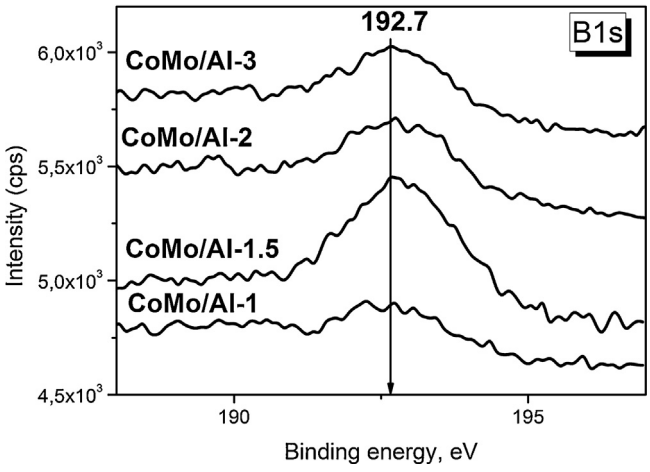

Fig. 7. XPS-spectra of B1s.

characterized for S^{2-} and S_2^{2-} that are typical for sulfur in sulfide surrounding in Co-Mo catalysts [42,49].

B1s spectra of B-containing catalysts have the one peak at BE = 192.7 eV. Resulting BE value is lower than typical one for B_2O_3 with BE = 193.3 eV [51]. Lower BE value can be accounted for by interaction of boron with γ-Al_2O_3. Intensity of peaks differs (Fig. 7). The spectrum of CoMo/Al-1.5 contains the most intensive peak. It indicates that boron is better distributed on the alumina as compared to other catalysts. CoMo/Al-3 has the least intensity of B1s peak. It can be accounted for by segregation of boron particles on catalyst surface or by introduction of boron into alumina lattice.

4.4. IR-spectroscopy

Fig. 8 shows the IR spectra of pure γ-Al_2O_3 and aluminas modified by boron in the region of the stretching vibrations of OH groups. Before addition of boric acid, the main vibration bands are observed at 3790, 3775, 3755, 3730, and 3685 cm^{-1}. These bands are characterized for isolated Al—OH groups present on the alumina surface in different environments. The broad band at 3500–3600 cm^{-1} is assigned to hydrogen-bonded hydroxyl groups. Increase of boron loading results in a gradual decrease in the integrated intensity of bands of OH-groups. In addition, there is an appearance of a new sharp band at ca. 3695 cm^{-1}. The latter can be attributed to the stretching vibration of surface B—OH groups [52,53]. Addition of 1–2 wt.% of boron results in the decrease of integral intensity of bands at 3685 and 3730 cm^{-1} that is characterized for weak acidic bridging $Al^{VI}(OH)Al^{IV}$ and $Al^{VI}(OH)Al^{VI}$ groups [54]. The integral intensity of terminal Al—OH bands with frequency ν_{OH} = 3755–3790 cm^{-1} changes slightly. Such groups possess basic properties. There are a significant decrease of quantity of Al-O(H)-Al bridged band at ν_{OH} 3660–3730 cm^{-1} and disappearance of Al^{V}-OH terminal band at ν_{OH} 3775 cm^{-1} for CoMo/Al-3.

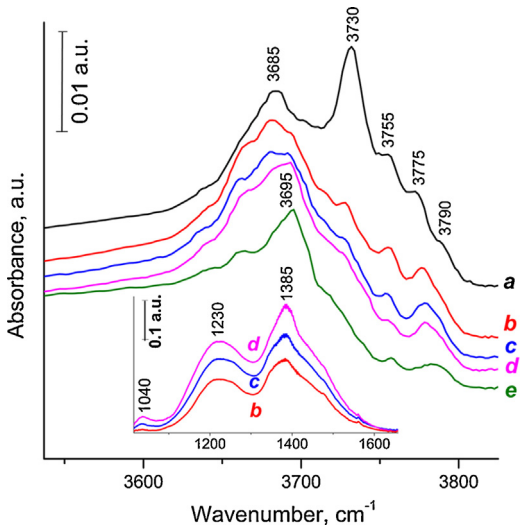

Fig. 8. IR spectra of boron modified alumina in the OH region: (a) Al_2O_3, (b) 1%B/Al_2O_3, (c) 1.5%B/Al_2O_3, (d) 2%B/Al_2O_3, and (e) 3%B/Al_2O_3. All spectra are background subtracted.

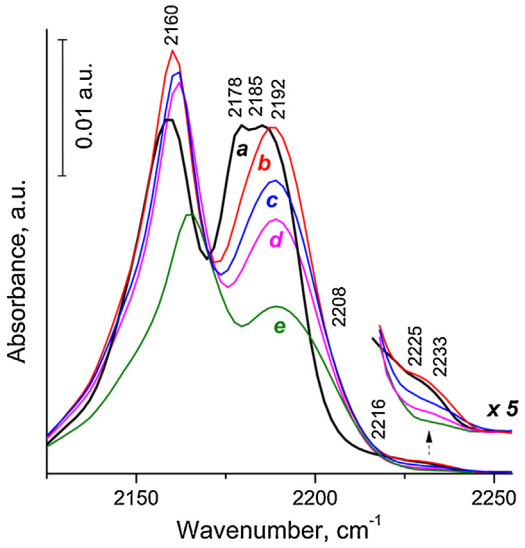

Fig. 9. IR spectra of CO adsorbed on boron modified aluminas at −196 °C and a CO pressure of 4 mbar: (a) Al_2O_3, (b) 1%B/Al_2O_3, (c) 1.5%B/Al_2O_3, (d) 2%B/Al_2O_3, and (e) 3%B/Al_2O_3. All spectra are background subtracted.

The IR spectra of supports show that boron addition results in a gradual increase of the two strong broad bands at 1230 and 1385–1450 cm^{-1} and week peak at 1040 cm^{-1} (Fig. 7, inset). According to Refs. [55,56], the broad peaks could be attributed to BO_3 trigonal surrounding and the small one to BO_4 tetrahedral surrounding. The higher intensity and broadness of the bands at 1230 and 1385–1450 cm^{-1} indicate that BO_3 surrounding are prevalent. Both kinds of species increased with growth of boron content.

The spectra of adsorbed CO on supports at 4 mbar are given in Fig. 9. Surface of alumina support without boron showed adsorption bands that corresponds to Lewis sites: band at 2233 and 2225 cm^{-1} relating to CO complexes with strong LAS; band at 2216 cm^{-1} is

Table 4
Type of acid sites, their concentration (μmol/g) and strength according to FTIR of adsorbed CO.

Type of sites	Lewis acid sites				Brønsted acid sites
	Strong	Medium I	Medium II	Week	Medium
ν (cm^{-1})	ν_{CO} = 2233–2225	ν_{CO} = 2215	2208	ν_{CO} = 2192–2178	ν_{OH} = 3690
The strength of sites[a]	Q_{CO} = 56.5–51.5	Q_{CO} = 46.5	Q_{CO} = 43	Q_{CO} = 35–27	$\Delta\nu_{OH}$ = 210
Sample	Concentration (μmol/g)				%
Al_2O_3	9	11	–	760	–
1%B-Al_2O_3	10	10	100	690	–
1.5%B-Al_2O_3	6	10	100	570	80
2%B-Al_2O_3	4	7	95	470	95
3%B-Al_2O_3	2	7	94	310	100

[a] Q_{CO}—heat of adsorption, kJ/mol, $\Delta\nu_{OH}$—the shift of IR band of the acidic hydroxyls due to interaction with adsorbed CO molecules, cm^{-1}.

characterized medium LAS, and peaks at 2185 and 2178 cm^{-1} are corresponded to week LAS. The strong LAS relating to CO complexes with Al^{3+} ions in pentahedron environment and the weak LAS at ν_{CO} = 2185 cm^{-1} can be attributed to CO complexes with Al^{3+}ions in octahedral environment, which are located to extended alumina crystals edges. The band at ν_{CO} = 2178 cm^{-1} is probably related to CO adsorption on Na^+ mixture ions. The low-frequency peak at 2160 cm^{-1} is characterized CO complexes with Al-OH bands. Supporting of 1 wt.% of boron results in significant changes of the spectrum of adsorbed CO. The intensity decrease of the band at 2178 cm^{-1} and shift of the position of peak maximum at 2185 cm^{-1} to higher frequencies (to 2192 cm^{-1}) indicates of strength increase of LAS by 3–4 kJ/mol. New band at ν_{CO} = 2208 cm^{-1} appears for CoMo/Al-3, it is good accordance with Ref. [57] and corresponds to boron in tetrahedral coordination, because tetrahedral B, as in BPO_4 [57], can act as a very strong Lewis site. Concentrations of acid sites are given in Table 4. The increase of boron content results in gradual reduction of concentration of strong and weak LAS. It was noted that content of weak acid sites decreased due to the increase of alumina plane covering by boron oxide. Concentration of medium LAS changes insignificantly. Also it was noted that new band at 2172 cm^{-1} appeared for 1.5–3 wt.% of boron, which corresponded to CO complexes with acidic OH-groups.

The shift of surface hydroxyl groups to low frequency area after CO adsorption at 77 K is $\Delta\nu_{O-H\cdots CO}$ = 130–140 cm^{-1}. Addition of 1 wt.% of boron does not influence acidic properties of OH bands. However, when the 1.5–3 wt.% of boron is added, the peak at 3480 cm^{-1} will appear. This peak corresponds to the complexes of CO with B—OH bands. The shift value of hydroxyl band is $\Delta\nu_{O-H\cdots CO}$ = 210 cm^{-1} that corresponds to weak Brønsted acidic site (BAS).

4.5. Catalytic activity

CoMo/Al-0 has high activity in HDS and HDN of diesel fuel with 5 vol.% of catalytic cracking gasoil. Residual sulfur content in hydrotreating product is 28 ± 2 ppm at 340 °C. The same residual sulfur content was reached at temperatures of 340–360 °C.

CoMo/Al-x catalysts with boron superior in HDS and HDN to the catalyst without boron (Fig. 10). High activity in HDN of the catalysts with boron was attained at 340 °C. Residual nitrogen content in this case is 7 ± 2 ppm. Increase of a temperature does not result in significant HDN activity growth. For all conditions, catalysts can be set in following order: CoMo/Al-1 < CoMo/Al-3 < CoMo/Al-2 < CoMo/Al-1.5. Consequently, CoMo/Al-1.5 has the highest activity in HDN.

The catalysts have similar activity in HDS at 340 °C. Increase of a temperature results activity growth. CoMo/Al-2 provided residual sulfur content less than 10 ppm at 350 °C. While other catalysts attained this activity level at 360 °C.

Comparison of B-containing catalysts showed that CoMo/Al-2 combined high activity in HDS and HDN.

5. Discussion

Hydrotreating catalysts with alumina supports are traditional systems. This type of catalysts is widely used in industrial scale. However, the search for ways to a further development does not stop because of rising necessity to improve their performance. Researches pay a great attention to investigation of boron influence on properties of hydrotreating catalysts. It is caused by availability and low cost of boron precursors, while positive effect on catalytic activity is high. Numerous studies of boron influence on catalytic activity showed that addition of boron results in changing dispersity of active component, its morphology, acidic properties of supports and catalysts and etc. Changing of acidic properties of the support should influence distribution of active phase in catalyst grain. Thus, it was shown in Refs. [58,59] that, depending on support properties, active component of hydrotreating catalysts can be distributed differently. Moreover, distribution of active metals can be effected by preparation method, namely duration of impregnation, impregnation technique and composition of impregnation solution [60,61]. Recently, it was shown that catalyst preparation method used in present paper provided uniform impregnation of support granules by solution of bimetallic complex compound [36,37,62]. Moreover, application of bimetallic complex as a precursor of active component ensures selective synthesis of high active CoMoS phase. In present work, the preparation method provided uniform impregnation of catalysts granules independently to boron content. It was confirmed by even coloring of granules in solution color. However, uniform coloring does not indicate that boron has no influence on conversion of active metal at other preparation stages.

Indirect confirmation of the uniform distribution of the active component in the granule can be obtained from textural characteristics of the supports and catalysts. Textural characteristics of the supports showed that addition of the boron had slight influence on surface area and pore volume of the supports and catalysts. It was shown in Ref. [18] that addition of boron causes insignificant decrease of surface area of the supports and then catalysts. The authors attributed this affect to dissolution of the pore walls by boric acid or blocking of micropores by bulk particles of B_2O_3 at 2 wt.% of B. In this paper, the opposite effect is observed. There is the slight increase in the specific surface area at 3 wt.% of B in paste of support. The conclusion can be made due to the absence of micropores in initial supports that increase of surface is attributed to incorporation of B particles between alumina particles. Nevertheless, no plugging of pores was observed. It is confirmed by preservation of the shape of adsorption-desorption isotherms. According to pore size distributions, localization of active component is uniform in the entire range of pore presence independently

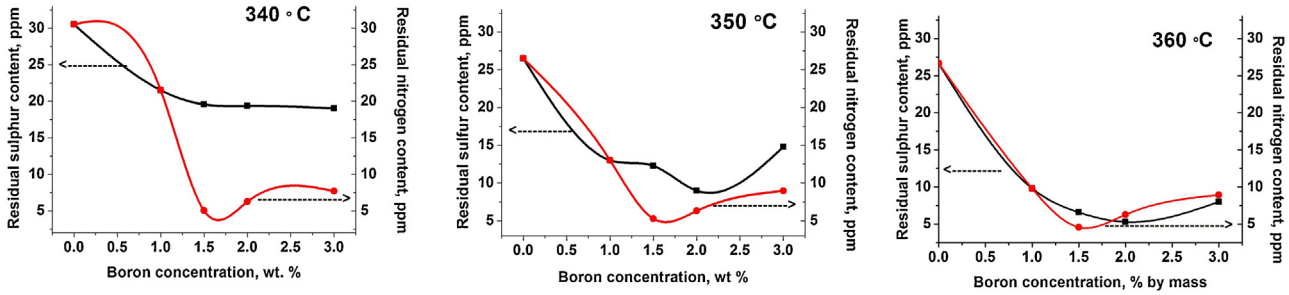

Fig. 10. Residual sulfur and nitrogen content for samples CoMo/Al-x.

Table 5
Atomic Co/Mo ratio according to XPS data.

Sample catalyst	Co/Mo
CoMo/Al-0	0.16
CoMo/Al-1	0.30
CoMo/Al-1.5	0.29
CoMo/Al-2	0.26
CoMo/Al-3	0.30

to boron content. In general, it can be concluded that boron incorporation did not practically influence on textural characteristics of the catalysts.

Synthesis of active component in the form of fully sulfide bimetallic particles (CoMoS phase of Type II) is important question for production of high active CoMo-catalysts for hydrotreating of diesel fuels [1,3–7]. In present work, the binding energies from Mo3d, Co2p and S2p spectra are well agrees with the literature data for CoMoS phase [11,42,46,48–50]. Resulting values for the $\Delta BE_{Co2p\text{-}Mo3d} = 549.9$ eV and $\Delta BE_{Co2p\text{-}S2p} = 617.3$ eV (Table 3) are also in a good accordance with the literature data [47,49] for CoMoS phase. Besides, it was found in Ref. [49] for supported sulfide CoMo-catalysts, that the atomic ratio of Co/Mo less than 0.5 indicated the formation of the fully sulfide CoMoS particle. In present work, the ratio of Co/Mo is equal to 0.3 for all prepared catalysts (Table 5) that indirectly confirms preferential formation of the sulfide active component. Deconvolution of Mo3d spectra for all samples showed that content of CoMoS phase was 70–89%. According to deconvolution of Co2p spectra, content of CoMoS is 58–75 %. Considerable difference in cobalt content in the composition of CoMoS phase is caused by low intensity of bands in the spectra. It results in rather high inaccuracy of definition of cobalt content during spectra deconvolution. However, resulting values are typical for highly active hydrotreating catalysts that contain no individual sulfides [49]. Thus, it is possible to claim that the formation of CoMoS phase occurs for all prepared catalysts. Consequently, the addition of boron into a support does not results in segregation of active metals into individual sulfides.

HRTEM data showed that an average slab length of active component changed from 3.1 to 3.8 nm depending on a boron content. The resulting length is typical for MoS_2 particles in highly active hydrotreating catalysts [63,64]. Usman et al. [65] showed that addition of boron causes increase if average slab length. According to HRTEM and NO adsorption data, the authors concluded that there was no increase of promotion of MoS2 particles by cobalt with the increase of slab length. Moreover, it caused decrease of catalytic activity at B content more than 0.6 wt.%. In present work, there is the increase of catalytic activity at addition of 2 wt.% of B. Further increase of boron content resulted in catalytic activity decrease. At the same time, average slab length increases significantly at 1 wt.% of B and then monotonously decreases at higher content. It is noted that the most active catalysts (1.5 and 2 wt.% B) have similar slab length of active component. Consequently, it can be concluded that there is the formation of active component with optimal covering CoMoS phase by cobalt at these boron contents.

There is no changing of stacking number of active component in the catalysts with boron, while average slab length increases. Active component in all catalysts is preferentially has one layer in the slab. It can be proposed that presence of monolayer particles of active component, which are located parallel to support surface, can result in formation of CoMoS phase of Type I. Therefore, addition of boron to Al_2O_3 should increase the intrinsic activity by conversion of CoMoS phase of Type I to pseudo-Type II by reducing the interactions between the support-MoS_2 particles [65]. However, previously it was shown [36,37] that preparation of catalysts from bimetallic complex compounds ensured the formation of CoMoS phase of Type II due to the presence of carbon deposits. These carbon deposits are formed by decomposition of chelating ligands and localized between active component and support. Therefore, catalysts contain monolayer slabs of CoMoS phase of Type II independently to boron content.

However, in the case of boron addition to paste of the support, increase of visualization degree of active component particles was observed while stacking degree remained unchanged. The results of Ref. [66] showed that single-layered particles of CoMoS phase, which were oriented parallel to support surface, should have low activity in HDS reactions. It is caused by the fact that most part of active component particle is basal plane of MoS_2 that is practically inactive in HDS reactions. Therefore, increase of visualization degree due to B addition should have positive effect on catalytic activity. Indeed, the catalysts with B have significantly higher activity in HDS and HDN reactions. Consequently, if active component in catalysts with different B content has similar stacking degree and different slab length and visualization degree, changing acidic properties of the support will be expected to occur. These acidic properties will influence «not parallel to the surface of a support» orientation of active component particles.

Therefore, the catalysts contain active component with the same composition and morphology and different texture. However, their catalytic activity differs significant. It is likely that changes in activity after boron incorporation occur due to alterations of acidic properties of the supports. Morphology of active component of boron catalysts differs from morphology of the catalysts without boron. Supposal can be made that boron results in the formation of new acidic sites. Nature of these sites decreases interaction between active component and a support.

On basis of IR-spectroscopy data, there are changes in OH groups that agrees with [53,55]. Consequently, B compounds react with almost types of Al—OH surface groups during the preparation of molding paste, probably via Al—O—B bridges, that leads to the formation of surface B—OH groups. These Al—O—B bridges are responsible for stabilization of an over-layer of boron species on the surface of alumina. It was found in Ref. [14] that MoO_3 particles

interacted with hydroxyl groups of a support during impregnation. Indeed, concentration of Al—OH bands decreases and B-OH forms, when boron content is more than 0.6 wt.%. Generation of surface B—OH groups leads to the decrease in interaction between active component and a support. In present work, it is supposed that generation of B—OH groups leads to an increase or "not-parallel-to-the-support" orientation of active component particles. In addition, bands, which correspond to the formation of trigonal and tetrahedral oxide surroundings of boron, were found. Two strong wide peaks observed at ν_{CO} = 1230 cm^{-1} and ν_{CO} = 1385–1450 cm^{-1} that corresponded to oxide boron surrounding [24,55,56]. The band at ν_{CO} = 2208 cm^{-1} from BO_4 surrounding [32,57], appeared while boron concentration was more than 3 wt.%. Observed data are in good accordance with Ref. [32], where trigonal boron oxide surrounding were found to form at low boron content. Tetragonal boron oxide surrounding is formed at boron content more than 2 wt.%. Thus, IR-spectroscopy of adsorbed CO showed that 1.5–3 wt.% of boron in a support resulted in generation of middle BAS, that agreed with Refs. [13,24,67].

Therefore, the increase of catalytic activity after addition of 1–3 wt.% of boron can be accounted for by the formation of new surface acid B—OH groups. It causes the formation of large amount of BAS and LAS of middle strength. It is stated in Ref. [68] that there is also dependence of activity on density of acid sites. The higher density of acid sites, the higher catalytic activity. Simultaneously, the increase of visualization degree and average slab length of active component particles occurs with the increase of density of acid sites. Therefore, changing surface properties of initial supports cause increase of "not parallel to the support" particles of active component while stacking degree remains unchanged. At the same time, the higher content of B, the higher visualization degree. Therefore, the increase of catalytic activity occurs due to the increase of amount of single-layered active component particles into reaction.

In present work, the higher amount of BAS and lower amount of LAS, the higher catalytic activity. It is caused by the fact that CoMo/Al-1.5 and CoMo/Al-2 have the highest density of BAS and the lowest of LAS in initial supports. However, CoMo/Al-2 catalyst is the most active, because it combines high activity in HDS and HDN reactions. This catalyst possesses the highest visualization degree and low slab length. Possibly, such characteristics result in optimal decoration degree of active component by cobalt, while amount of single-layered "not parallel to the support" oriented particles of CoMoS phase is maximal.

6. Conclusion

CoMo catalysts with different amount of boron in the supports were studied. Content of a boron in supports was 0, 1, 1.5, 2 and 3 wt.%. All supports and catalysts were studied by nitrogen adsorption-desorption, IR of adsorbed CO, XPS and HRTEM. It was shown that addition of boron had no significant influence on textural characteristics of the supports and catalysts and morphology of active component. However, it was noted that addition of boron into the support resulted in changing acidic properties. In particularly, there are the increase of the amount of middle BAS and decrease of middle LAS. Also addition of 1–3 wt.% of boron causes the formation of new surface acid B—OH groups. Changing acidic properties of the support ensure the increase of visualization degree and average slab length that causes increase of amount of "not parallel to the support" oriented particles of CoMoS phase with the highest activity. Therefore, boron addition has a positive influence on catalytic activity. It was shown that CoMo catalyst with 2 wt.% of boron in the paste of the support had the highest activity in hydrodesulfurization of diesel fuel with addition of cracking gasoil.

Acknowledgement

The work was supported by Ministry of Education and Science of the Russian Federation: Project No. 14.610.21.0008, identification number of the project RFMEFI61015X0008.

References

[1] J.V. Lauritsen, J. Kibsgaard, G.H. Olesen, P.G. Moses, B. Hinnemann, S. Helveg, J.K. Nørskov, B.S. Clausen, H. Topsøe, E. Lægsgaard, F. Besenbacher, J. Catal. 249 (2007) 220–233.
[2] M. Breysse, J.L. Portefaix, M. Vrinat, Catal. Today 10 (1991) 489–505.
[3] Y. Okamoto, K. Hioka, K. Arakawa, T. Fujikawa, T. Ebihara, T. Kubota, J. Catal. 268 (2009) 49–59.
[4] S.M.A.M. Bouwens, F.B.M. Vanzon, M.P. Vandijk, A.M. Vanderkraan, V.H.J. Debeer, J.A.R. Vanveen, D.C. Koningsberger, J. Catal. 146 (1994) 375–393.
[5] M. Brorson, A. Carlsson, H. Topsøe, Catal. Today 123 (2007) 31–36.
[6] H. Topsøe, Appl. Catal. A 322 (2007) 3–8.
[7] H. Topsøe, B. Hinnemann, J.K. Nørskov, J.V. Lauritsen, F. Besenbacher, P.L. Hansen, G. Hytoft, R.G. Egeberg, K.G. Knudsen, Catal. Today 107–108 (2005) 12–22.
[8] M. Breysse, P. Afanasiev, C. Geantet, M. Vrinat, Catal. Today 86 (2003) 5–16.
[9] J. Ramirez, S. Fuentes, G. Díaz, M. Vrinat, M. Breysse, M. Lacroix, Appl. Catal. 52 (1989) 211–224.
[10] F.E. Massoth, G. Muralidhar, J. Shabtai, J. Catal. 85 (1984) 53–62.
[11] O.V. Klimov, K.A. Leonova, G.I. Koryakina, E.Y. Gerasimov, I.P. Prosvirin, S.V. Cherepanova, S.V. Budukva, V.Y. Pereyma, P.P. Dik, O.A. Parakhin, A.S. Noskov, Catal. Today 220–222 (2014) 66–77.
[12] G. Muralidhar, F.E. Massoth, J. Shabtai, J. Catal. 85 (1984) 44–52.
[13] V.-G. Baldovino-Medrano, A. Centeno, S.-A. Giraldo, Cien. Tecnol. Futuro 4 (2010) 91–99.
[14] U. Usman, M. Takaki, T. Kubota, Y. Okamoto, Appl. Catal. A 286 (2005) 148–154.
[15] M. Lewandowski, Z. Sarbak, Fuel 79 (2000) 487–495.
[16] D. Li, T. Sato, M. Imamura, H. Shimada, A. Nishijima, Appl. Catal. B 16 (1998) 255–260.
[17] F. Rashidi, T. Sasaki, A.M. Rashidi, A. Nemati Kharat, K.J. Jozani, J. Catal. 299 (2013) 321–335.
[18] J. Ramírez, P. Castillo, L. Ceden˜o, R. Cuevas, M. Castillo, J. Palacios, A. López-Agudo, Appl. Catal. A 132 (1995) 317–334.
[19] D. Li, T. Sato, M. Imamura, H. Shimada, A. Nishijima, J. Catal. 170 (1997) 357–365.
[20] P. Torres-Mancera, J. Ramírez, R. Cuevas, A. Gutiérrez-Alejandre, F. Murrieta, R. Luna, Catal. Today 107–108 (2005) 551–558.
[21] W. Chen, F. Maugé, J. van Gestel, H. Nie, D. Li, X. Long, J. Catal. 304 (2013) 47–62.
[22] G.M. Dhar, B.N. Srinivas, M.S. Rana, M. Kumar, S.K. Maity, Catal. Today 86 (2003) 45–60.
[23] A.M.D. de Farias, A.M.L. Esteves, F. Ziarelli, S. Caldarelli, M.A. Fraga, L.G. Appel, Appl. Surf. Sci. 227 (2004) 132–138.
[24] F.M. Bautista, J.M. Campelo, A. Garcia, D. Luna, J.M. Marinas, M.C. Moreno, A.A. Romero, J.A. Navio, M. Macias, J. Catal. 173 (1998) 333–344.
[25] L. Ding, Z. Zhang, Y. Zheng, Z. Ring, J. Chen, Appl. Catal. A 301 (2006) 241–250.
[26] Usman, T. Kubota, I. Hiromitsu, Y. Okamoto, J. Catal. 247 (2007) 78–85.
[27] H. Lafitau, E. Neel, J.C. Clement, Physico-chemical interaction between Ni and support in the preparation of Ni-Mo/Al203 hydrogenolysis catalystsa, in: P.J.B. Delmon, G. Poncelet (Eds.), Studies in Surface Science and Catalysis, Elsevier, 1976, pp. 393–404.
[28] M. Houalla, B. Delmon, Appl. Catal. 1 (1981) 285–289.
[29] M.A. Stranick, M. Houalla, D.M. Hercules, J. Catal. 104 (1987) 396–412.
[30] Y. Izumi, T. Shiba, Bull. Chem. Soc. Jpn. 37 (1964) 1797–1809.
[31] C. Li, Y.W. Chen, S.J. Yang, J.C. Wu, Ind. Eng. Chem. Res. 32 (1993) 1573–1578.
[32] S. Sato, M. Kuroki, T. Sodesawa, F. Nozaki, G.E. Maciel, J. Mol. Catal. A: Chem. 104 (1995) 171–177.
[33] J. Zheng, Z. Xia, J. Li, W. Lai, X. Yi, B. Chen, W. Fang, H. Wan, Catal. Commun. 21 (2012) 18–21.
[34] J.-L. Dubois, S. Fujieda, Catal. Today 29 (1996) 191–195.
[35] F.S. Mederos, J. Ancheyta, J. Chen, Appl. Catal. A 355 (2009) 1–19.
[36] O.V. Klimov, A.V. Pashigreva, G.A. Bukhtiyarova, S.V. Budukva, M.A. Fedotov, D.I. Kochubey, Y.A. Chesalov, V.I. Zaikovskii, A.S. Noskov, Catal. Today 150 (2010) 196–206.
[37] O.V. Klimov, A.V. Pashigreva, M.A. Fedotov, D.I. Kochubey, Y.A. Chesalov, G.A. Bukhtiyarova, A.S. Noskov, J. Mol. Catal. A: Chem. 322 (2010) 80–89.
[38] E.A. Paukshtis, E.N. Yurchenko, Russ. Chem. Rev. 52 (1983) 242–258.
[39] R.I. Soltanov, E.A. Paukshtis, E.N. Yurchenko, Kinet. Catal. 23 (1982) 135–141.
[40] K.P. de Jong, General Aspects, Synthesis of Solid Catalysts, Wiley-VCH Verlag GmbH & Co. KGaA, 2009, p. 402.
[41] M. Thommes, K. Kaneko, A.V. Neimark, J.P. Olivier, F. Rodriguez-Reinoso, J. Rouquerol, K.S.W. Sing, Pure Appl. Chem. 87 (2015) 1051–1069.
[42] D. Laurenti, B. Phung-Ngoc, C. Roukoss, E. Devers, K. Marchand, L. Massin, L. Lemaitre, C. Legens, A.-A. Quoineaud, M. Vrinat, J. Catal. 297 (2013) 165–175.
[43] H. Topsøie, R. Candia, N.-Y. Topsøe, B.S. Clausen, H. Topsøe, Bull. Soc. Chim. Belg. 93 (1984) 783–806.

[44] J.A.R. van Veen, E. Gerkema, A.M. van der Kraan, A. Knoester, J. Chem. Soc.: Chem. Commun. (1987) 1684–1686.
[45] C.-E. Xiang, Y.-M. Chai, J. Fan, C.-G. Liu, J. Fuel Chem. Technol. 39 (2011) 355–360.
[46] J.S. Brinen, W.D. Armstrong, J. Catal. 54 (1978) 57–65.
[47] N. Frizi, P. Blanchard, E. Payen, P. Baranek, C. Lancelot, M. Rebeilleau, C. Dupuy, J.P. Dath, Catal. Today 130 (2008) 32–40.
[48] J.H. Scofield, J. Electron. Spectrosc. Relat. Phenom. 8 (1976) 129–137.
[49] A.D. Gandubert, E. Krebs, C. Legens, D. Costa, D. Guillaume, P. Raybaud, Catal. Today 130 (2008) 149–159.
[50] J.A. Toledo-Antonio, M.A. Cortés-Jácome, C. Angeles-Chávez, J. Escobar, M.C. Barrera, E. López-Salinas, Appl. Catal. B 90 (2009) 213–223.
[51] E.A. Il'inchik, V.V. Volkov, L.N. Mazalov, J. Struct. Chem. 46 (2016) 523–534.
[52] M.J.D. Low, N. Ramasubramanian, J. Phys. Chem. 70 (1966) 2740–2746.
[53] M. Sibeijn, J.A.R. Vanveen, A. Bliek, J.A. Moulijn, J. Catal. 145 (1994) 416–428.
[54] E.A. Paukshtis, P.I. Soltanov, E.N. Yurchenko, K. Jirátová, Collection Czechoslov. Chem. Commun. 47 (1982) 2044–2060.
[55] D.J. Perez Martinez, G.A. Acevedo Quiroga, S.A.G. Duarte, A.C. Hurtado, Rev. Fac. Ing. Univ. Antioq. 57 (2011) 23–30.
[56] A. Delmastro, G. Gozzelino, D. Mazza, M. Vallino, G. Busca, V. Lorenzelli, J. Chem. Soc.: Faraday Trans. 88 (1992) 2065–2070.
[57] T. Sanders, J.B. Moffat, J. Colloid Interface Sci. 120 (1987) 451–455.
[58] K. Soukup, M. Procházka, L. Kaluža, Chem. Eng. Trans. 43 (2015) 841–846.
[59] L. Kaluža, M. Zdražil, Catal. Lett. 127 (2009) 368–376.
[60] M.A. Goula, C. Kordulis, A. Lycourghiotis, J. Catal. 133 (1992) 486–497.
[61] M.A. Goula, C. Kordulis, A. Lycourghiotis, J.L.G. Fierro, J. Catal. 137 (1992) 285–305.
[62] A.V. Pashigreva, O.V. Klimov, G.A. Bukhtiyarova, D.I. Kochubey, I.P. Prosvirin, Y.A. Chesalov, V.I. Zaikovskii, A.S. Noskov, Catal. Today 150 (2010) 164–170.
[63] S. Eijsbouts, J.J.L. Heinerman, H.J.W. Elzerman, Appl. Catal. A: Gen. 105 (1993) 53–68.
[64] S. Eijsbouts, J.J.L. Heinerman, H.J.W. Elzerman, Appl. Catal. A 105 (1993) 69–82.
[65] Usman, T. Kubota, Y. Araki, K. Ishida, Y. Okamoto, J. Catal. 227 (2004) 523–529.
[66] H. Shimada, Catal. Today 86 (2003) 17–29.
[67] D. Pérez Martínez, A.M. Lozano, C.J. Arias, V.C. Porras, G.A. Olarte, S.A. Giraldo, A. Centeno, Rev. Colomb. Quím. 37 (2008) 219–231.
[68] C. Flego, V. Arrigoni, M. Ferrari, R. Riva, L. Zanibelli, Catal. Today 65 (2001) 265–270.